

Experimental Evidence for Giant Vortex States in a Mesoscopic Superconducting Disk

A. Kanda,^{1,*} B. J. Baelus,^{2,3,†} F. M. Peeters,³ K. Kadowaki,² and Y. Ootuka¹

¹*Institute of Physics and Tsukuba Research Center for Interdisciplinary Material Science (TIMS),
University of Tsukuba, Tsukuba 305-8571, Japan*

²*Institute of Materials Science, University of Tsukuba, Tsukuba 305-8573, Japan*

³*Departement Fysica, Universiteit Antwerpen (Campus Drie Eiken),
Universiteitsplein 1, B-2610 Antwerpen, Belgium*

(Dated: November 13, 2018)

Response of a mesoscopic superconducting disk to perpendicular magnetic fields is studied by using the multiple-small-tunnel-junction method, in which transport properties of several small tunnel junctions attached to the disk are measured simultaneously. This allows us for the first experimental distinction between the giant vortex states and multivortex states. Moreover, we experimentally find magnetic field induced rearrangement and combination of vortices. The experimental results are well reproduced in numerical results based on the nonlinear Ginzburg-Landau theory.

The appearance of vortices in various quantum systems, such as superconductors, superfluids and Bose-Einstein condensates, is an intriguing phenomenon in nature. A conventional quantum vortex is singly quantized, having a core where the value of the order parameter decreases to zero, while its phase changes by 2π when encircling the core. Recently, an important breakthrough was established by the observation of doubly quantized vortex lines in superfluid ^3He -A[1]. For superconductors expectations are even more spectacular. In macroscopic type-II superconductors a triangular lattice of single flux quanta is formed, whereas two kinds of fundamentally new vortex states have theoretically been predicted in mesoscopic superconductors where the sample size approaches the size of Cooper-pairs[2, 3, 4, 5]; (i) multivortex states (MVSs) with a unique spatial arrangement of singly quantized vortices, and (ii) multiply quantized or giant vortex states (GVSs) with a single core in the center[6, 7].

Although several experimental techniques have been developed for observing these novel states[7, 8, 9, 10, 11, 12, 13], none of them has been able to make a clear distinction between MVSs and GVSs. In this Letter, we present the first experimental evidence for the existence of GVSs and MVSs in a circular disk, and demonstrate magnetic-field induced MVS-GVS and MVS-MVS transitions. Our results are in good agreement with the theoretical prediction based on the nonlinear Ginzburg-Landau (G-L) theory.

Here we used the multiple-small-tunnel-junction (MSTJ) method, in which several small tunnel junctions with high tunnel resistance are attached to a mesoscopic superconductor to simultaneously detect small changes in the local density of states (LDOS) under the junctions[14, 15]. Since the LDOS depends on the local supercurrent density, the MSTJ method gives us information on the distribution of the supercurrent, which reflects the detailed vortex structure inside the disk.

Figure 1 shows a schematic drawing and a scanning electron microscopy (SEM) image of the sample. Four

normal-metal (Cu) leads are connected to the periphery of the superconducting Al disk through highly resistive small tunnel junctions, A, B, C, and D. The sample is designed to be symmetrical with respect to the central axis SS' . The angles $\angle AOD$ and $\angle BOC$ are 120 and 32 degrees, respectively. Although junctions A and D and junctions B and C ideally have the same area and tunnel resistance, small differences actually exist between them. The normal-state tunnel resistance at 8 K was 40 and 33 k Ω for junctions A and D, and 17 and 25 k Ω for junctions B and C, respectively. The radius of the disk R was 0.75 μm and the disk thickness d was 33 nm. The disk was directly connected to an Al drain lead. To prevent oxidation of the disk in the air, we covered the Al surface with Ge (thickness: 28 nm), which becomes insulating at low temperatures [16]. All the above-mentioned processes were performed in a single vacuum with a base pressure of 2×10^{-8} Pa. The superconducting coherence length ξ was estimated to be 0.15 to 0.19 μm from the residual resistance of the Al films prepared in the same way. The superconducting transition temperature was 1.3 - 1.4 K.

In the measurement, we fixed the current flowing through each junction to a small value, typically 100 pA, and measured simultaneously the voltages between each of the four Cu leads and the drain lead, while sweeping the perpendicular magnetic field at a typical rate of 20 mT/min. Here, the current I is related to the voltage V through the superconducting LDOS N_s :

$$I = \frac{1}{eR} \int_0^{eV} \frac{N_s(E)}{N_n} dE \quad (\text{for } T \rightarrow 0), \quad (1)$$

where N_n is the normal density of states. Especially, at $T = 0$, $B = 0$ and $I \rightarrow 0$, $V = \Delta/e$. Variations in the LDOS are related to variations in the superconducting density $|\Psi|^2$.

Figures 2(a) and (c) show the change of the voltages at $I = 100$ pA in decreasing and increasing magnetic fields, respectively. V_A , V_B , V_C , and V_D denote the voltages at junctions A, B, C, and D, respectively. The magnetic-

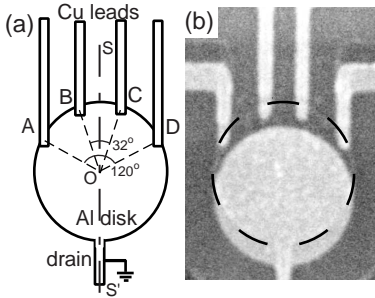


FIG. 1: Schematic view (a) and scanning electron micrograph (b) of our sample. Four normal-metal (Cu) leads are connected to the periphery of a superconducting Al disk (diameter = $1.5 \mu\text{m}$, thickness = 33 nm) through small tunnel junctions with area $\approx 0.01 (\mu\text{m})^2$. The disk is directly connected to an Al drain lead. This structure was fabricated using e-beam lithography followed by double-angle evaporation of Al and Cu. After the Al film was deposited, the surface of the Al film was slightly oxidized to provide the tunnel barrier. Most of the Al disk, indicated by the dashed circle, is covered with a Cu film (bright regions). We expect that the Cu film will not have any serious influence on the superconductivity of the Al disk because of the insulating AlO_x layer between them.

field dependence of the voltage originates from (i) smearing of the energy gap due to pair-breaking by the magnetic field, and (ii) a decrease of the energy gap because of the supercurrent [17].

The former leads to a moderate monotonic decrease in voltage as the strength of the magnetic field increases, so the rapid change in voltage comes from the latter. Especially, each voltage jump corresponds to a transition between different vortex states with a vorticity change of ± 1 [2, 3, 4]. This allows us to identify the vorticity L (the number of the flux quanta in the sample) as shown in each figure [18]. Note that the difference either between V_A and V_D or V_B and V_C at $B = 0$ mainly comes from a slight asymmetry in the junction resistance, which would also affect the characteristics in all magnetic-field ranges. To make voltage comparison easier, dV/dB is also displayed in Figs. 2(b) and (d).

Here, we focus on the features of the voltages in the symmetric junctions, V_A and V_D [19]. In decreasing magnetic field (Fig. 2(b)), remarkable differences are found in dV_A/dB and dV_D/dB for $L = 2$ and 4 to 11. This difference between dV_A/dB and dV_D/dB indicates that the supercurrent below junction A is essentially different from the one below junction D, which excludes an axially symmetric vortex distribution of the GVS and is characteristic of the MVS. This allows for an unparalleled determination of the magnetic field for which the vortex state is an MVS. For increasing magnetic fields (Fig. 2(d)), the difference in dV/dB is relatively large between $L = 4$ and 6, which is also due to the MVS formation.

This simple distinction between GVSs and MVSs is

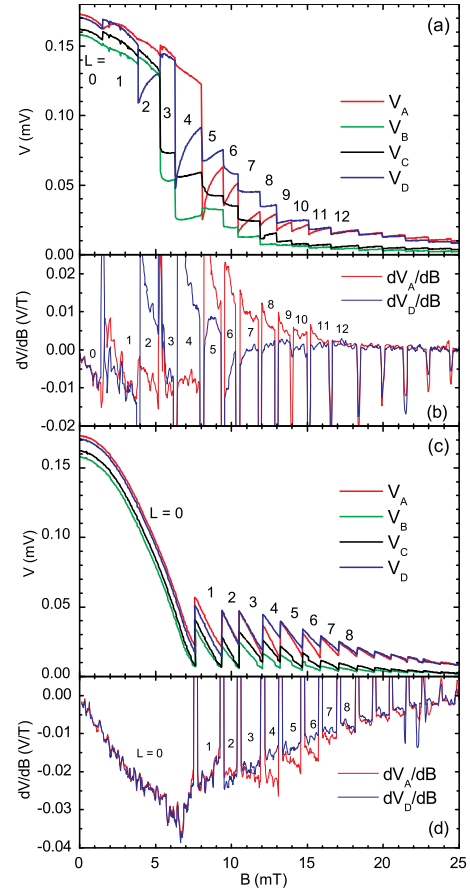


FIG. 2: (a) Variation of voltages at junctions A, B, C, and D in a decreasing magnetic field. The current through each junction is 100 pA . Temperature is 0.03 K . (b) Differential voltage dV/dB for junction pairs at symmetrical positions, A and D. (c)(d) The same as (a) and (b), respectively, but for increasing magnetic fields.

supported by a numerical simulation. Figure 3 shows the free energy for a disk with $R = 5.0\xi$, $d = 0.1\xi$, and the G-L parameter $\kappa = 0.28$ as calculated within the framework of the nonlinear G-L theory. This theoretical analysis is based on a fully self-consistent numerical solution of the coupled G-L equations, taking into account demagnetization effects. A more detailed description of the theoretical model can be found in Ref. [2]. The thickness was adjusted to obtain the best agreement with the experimentally obtained transition field between $L = 0$ and 1 states [15, 20]. Theoretically, MVSs nucleate for vorticity $L = 2$ to 10 for decreasing magnetic fields and $L = 3$ to 6 for increasing magnetic fields. Thus, the theoretical calculations confirm the identification of the GVS and MVS by the MSTJ method except for $L = 3$ ($L = 11$), where theoretically the state is predicted to be an MVS (GVS) while experimentally a GVS (MVS) was inferred.

The disagreement for $L = 3$ originates from the junction configuration. The contour plots in Fig. 3 show

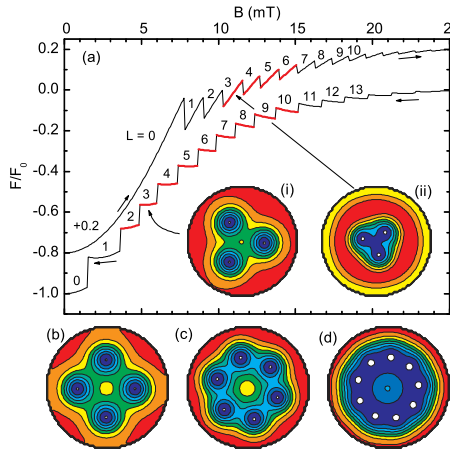


FIG. 3: (a) Calculated free energy F for a disk with $R = 5.0\xi$, $d = 0.1\xi$, and $\kappa = 0.28$, normalized by the $B = 0$ value F_0 , for decreasing and increasing magnetic fields. For the sake of clarity the free energy for increasing field is shifted over $+0.2F_0$. Red and black segments indicate MVS and GVS, respectively. The insets show the contour plots of the Cooper-pair density for the $L = 3$ state (i) at $B = 6.0$ mT and (ii) at $B = 11.0$ mT, corresponding to decreasing and increasing magnetic field, respectively. Red (blue) regions correspond to high (low) values of the Cooper-pair density. The Cooper-pair density for decreasing magnetic field is also shown for (b) the $L = 4$ state at $B = 7.2$ mT, (c) the $L = 6$ state at $B = 9.3$ mT, and (d) the $L = 9$ state at $B = 13.0$ mT.

examples of the theoretically expected vortex configuration for the MVSs. The $L = 3$ state (insets of Fig. 3(a)) has trigonal symmetry, which agrees with the angle $\angle AOD = 120$ degree. Thus, the voltage difference for the $L = 3$ MVS is significantly decreased for the A-D junction pair, concealing the $L = 3$ MVS. Although this kind of symmetry induced effect is also expected to appear in $L = 6$ and $L = 9$ MVSs (Figs. 3(c) and (d)), the dV/dB difference is significant for $L = 6$ and for $L = 9$, as shown in Figs. 2(b) and (d). The difference between the experiment and theory could be attributed to the effects of defects, i.e., the stabilization of a different vortex configuration or distortions of the vortex configurations caused by defects. Note that in such mesoscopic disks different vortex distributions with the same total vorticity L are possible [21]. For example, a state with L vortices on one shell or a state with $L - 1$ vortices on a shell and one in the center may become (meta-)stable. The free energy difference between such states with the same vorticity is very small and even the smallest defect (inside the disk or at the boundary of the disk) can influence the vortex distribution. The experimentally observed MVS for $L = 11$ could also be attributed to the effect of defects.

Actually, the influence of defects was noticeable for particular vorticities; e.g., for the $L = 0$ state in both Figs. 2(a) and (c), all curves are parallel to each other, showing that a uniform supercurrent is flowing along the

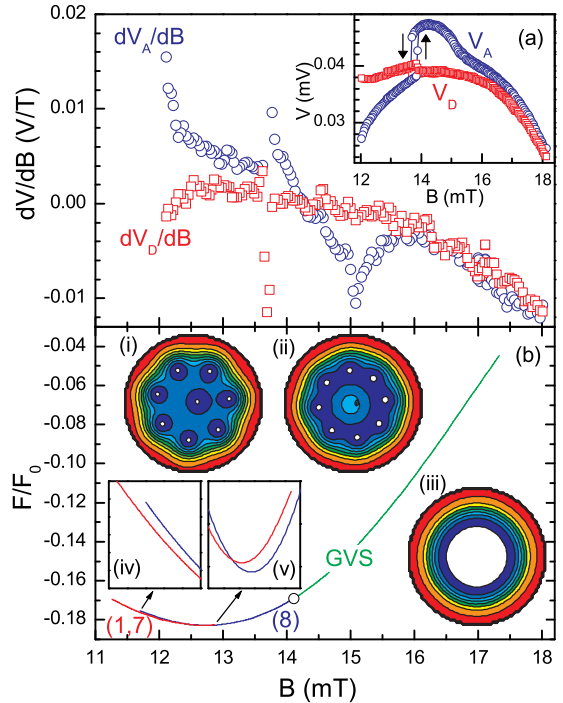


FIG. 4: (a) The main panel shows the differential voltages dV_A/dB and dV_D/dB for the $L = 8$ state in decreasing magnetic field. The inset shows the measured variation of voltages V_A and V_D for the $L = 8$ state. The arrows show the direction of the magnetic-field sweep. Small hysteresis is seen at the voltage jump (around 13.7 mT). (b) Comparison of the calculated free energy of the different (meta-) stable states with $L = 8$ as a function of the applied magnetic field; i.e., the (1,7)-state (red curve), the (8)-state (blue curve) and the GVS (green curve). To simulate a defect near the center, a circular hole with radius 0.1ξ is inserted at a distance 0.2ξ from the disk center. The insets (i)-(iii) present the Cooper-pair density of the (1,7) and the (8)-state at $B = 12.5$ mT, and the GVS at $B = 14.6$ mT. Insets (iv) and (v) show the transitions between the (1,7)-state and the (8)-state in more detail.

disk periphery. This means that there is no crucial defect *near the junctions*. On the other hand, for the $L = 1$ state, where only one vortex exists in the disk, curves are not exactly parallel. This indicates that the vortex is not exactly at the center of the disk, presumably because of a defect close to (but not at) *the disk center*. This will be confirmed in the discussion below. The small differences in vortex state transition fields between experiment and theory can also be attributed to the effect of defects [22].

In increasing magnetic fields, the dV/dB difference for MVS formation (Fig. 2(d)) is relatively small. This results from the position of the vortices. The vortices in increasing magnetic fields (e.g., inset (ii) of Fig. 3(a)) are situated more to the center in comparison with those for decreasing magnetic fields (e.g., inset (i) of Fig. 3(a)), leading to less variation of the supercurrent near the disk periphery. Similarly, we also attribute the smaller differ-

ences in dV/dB in MVSs with larger L (Fig. 2(b)) to less variation of the supercurrent along the disk periphery in comparison with smaller L , as shown in Figs. 3(b,c,d).

For $L = 2$ and $L = 7$ to 11, the type of the vortex state is different in decreasing and increasing magnetic fields. This implies the existence of a MVS-GVS transition at these vorticities, which has been predicted theoretically [2], but has never been observed experimentally. Figure 4(a) shows the entire $L = 8$ state, obtained by changing the sweep direction of magnetic field. The difference between dV_A/dB and dV_D/dB is remarkable below 15.8 mT, indicating that the state is an MVS, while at larger fields dV_A/dB and dV_D/dB coincide, indicating a GVS. Note that the observed MVS-GVS transition is a continuous one and is not accompanied by hysteresis, correspond to the theoretical prediction [2, 4]. Moreover, small voltage jumps with hysteresis observed around 13.7 mT [see the inset of Fig. 4(a)] indicate a transition between two vortex configurations with a different arrangement of the 8 vortices, which might be related to the presence of a defect near the sample center. For comparison, we calculated the different vortex configurations with $L = 8$ in a disk with a weak defect near the center (Fig. 4(b)). At low fields, we find two stable MVSs with $L = 8$; one is the (1,7)-state, in which 1 vortex exists near the center pinned by the defect and 7 vortices are located on a shell [inset (i)], and the other is the (8)-state, in which all 8 vortices are arranged on a shell [inset (ii)]. At higher fields the GVS with $L = 8$ is found to be most stable [inset (iii)]. With decreasing field the GVS transits into the (8)-state at $B = 14.1$ mT and then into the (1,7)-state at $B = 11.7$ mT. With increasing field the (1,7)-state transits into the (8)-state at $B = 12.9$ mT, and then into the giant vortex state at $B = 14.1$ mT. Note that the MVS-GVS transition at $B = 14.1$ mT is a continuous one (second order transition), in agreement with the experimental observation, while the transition between the two MVSs is discontinuous and hysteretic [see insets (iv) and (v) of Fig. 4(b)], as was also the case in the experiment [see the inset of Fig. 4(a)]. Also note that the (1,7)-state is theoretically stable only in the presence of weak defects, which is consistent with the observation in the $L = 1$ state, as discussed above.

Thus, the major experimental results for this particular disk are successfully explained by the calculation taking into account a single strong defect near the disk center. But as seen in the figures, small discrepancies exist in fields for transitions between different vortex states obtained in experiment and theory. Also, different disks with the same geometry have a little bit different transition fields [15]. These might come from a distribution of much weaker defects. Additional experiments on a number of similar disks will be required to resolve this matter. However, this is beyond the scope of the present letter.

In conclusion, we have studied the magnetic response of a mesoscopic superconducting disk by using the MSTJ

method. By comparing the voltages at symmetrical positions, we experimentally determine the type of vortex states: GVS or MVS. We also observed the MVS-MVS and MVS-GVS transitions with a fixed vorticity. The results agree with theoretical predictions based on the G-L theory.

Finally, we want to remark that our method can be applied to other geometries such as squares and triangles, in which antivortices might be stabilized for some vorticities [11, 12, 23, 24].

This work was partially supported by the University of Tsukuba Nanoscience Special Project, the 21st Century COE Program of MEXT, the JSPS Core-to-Core Program, the Flemish Science Foundation (FWO-Vl) and the Belgian Science Policy. B. J. B. acknowledges support from JSPS and FWO-Vl.

* kanda@lt.px.tsukuba.ac.jp

† ben.baelus@ua.ac.be

- [1] R. Blaauwgeers, *et al.* *Nature (London)* **404**, 471 (2000).
- [2] V. A. Schweigert *et al.*, *Phys. Rev. Lett.* **81** 2783 (1998).
- [3] J. J. Palacios, *Phys. Rev. B* **58** R5948 (1998).
- [4] J. J. Palacios, *Phys. Rev. Lett.* **84** 1796 (2000).
- [5] B. J. Baelus *et al.*, *Phys. Rev. B* **63** 144517 (2001).
- [6] V. V. Moshchalkov *et al.*, *Phys. Rev. B* **55**, 11793 (1997).
- [7] V. Bruyndoncx, *et al.*, *Phys. Rev. B* **60** 4285 (1999).
- [8] A. K. Geim *et al.*, *Nature (London)* **390** 259 (1997).
- [9] A. K. Geim *et al.*, *Nature (London)* **396** 144 (1998).
- [10] A. K. Geim *et al.*, *Phys. Rev. Lett.* **85** 1528 (2000).
- [11] L. F. Chibotaru *et al.* *Nature (London)* **408** 833 (2000).
- [12] L. F. Chibotaru *et al.* *Phys. Rev. Lett.* **86** 1323 (2001).
- [13] Y. Hata *et al.*, *Physica* **338-339C** 719 (2003).
- [14] A. Kanda and Y. Ootuka, *Microelectron. Eng.* **63** 313 (2002).
- [15] A. Kanda and Y. Ootuka, *Physica* **404C** 205 (2004).
- [16] The effect of the Ge layer on the Al surface oxidization has not been confirmed experimentally.
- [17] M. Tinkham, *Introduction to Superconductivity*, 2nd ed. (McGraw-Hill, New York, 1996), chap. 10.
- [18] Small voltage jumps in V_B at 0.010 mV and in V_C at 0.013 mV seen in Figs. 2(a) and (c) do not correspond to vortex state transitions, but are due to errors in the voltage measurement at these voltages, presumably because of change in the measurement range in our digital multimeters.
- [19] In V_B and V_C , the effects discussed in the text were less pronounced, presumably because of the short separation between the two leads.
- [20] The thickness used in the calculation corresponds to 15 to 19 nm. The difference from the actual thickness ($d = 33$ nm) probably comes from the film granularity and the surface oxide layer. [See, T. Wada *et al.* *J. Vac. Sci. Technol. A* **16** 1430 (1998).] The study of thickness dependence may make the origin of the discrepancy clear.
- [21] B. J. Baelus *et al.*, *Phys. Rev. B* **69** 064506 (2004).
- [22] G. M. Braverman *et al.*, *Phys. Rev. B* **59** 12039 (1999).
- [23] J. Bekaert *et al.*, *Physica* **404C** 44 (2004).
- [24] M. Morelle *et al.*, cond-mat/0407061.